

***In vitro* and *in vivo* degradation of non-woven materials made of poly(ϵ -caprolactone) nanofibers prepared by electrospinning under different conditions**

N. BÖLGEN¹, Y. Z. MENCELOĞLU², K. ACATAY², İ. VARGEL³
and E. PIŞKIN^{1,*}

¹ *Hacettepe University, Chemical Engineering Department and Bioengineering Division and TÜBİTAK-ÜSAM-Biyomedek, Beytepe, Ankara, Turkey*

² *Sabancı University, Faculty of Engineering and Natural Sciences, Tuzla, Istanbul, Turkey*

³ *Hacettepe University, Faculty of Medicine, Department of Plastic and Reconstructive Surgery, Ankara, Turkey*

Received 25 January 2005; accepted 21 May 2005

Abstract—The aim of this study was to prepare non-woven materials from a biodegradable polymer, poly(ϵ -caprolactone) (PCL) by electrospinning. PCL was synthesized by ring-opening polymerization of ϵ -caprolactone in bulk using stannous octoate as the catalyst under nitrogen atmosphere. PCL was then processed into non-woven matrices composed of nanofibers by electrospinning of the polymer from its solution using a high voltage power supply. The effects of PCL concentration, composition of the solvent (a mixture of chloroform and DMF with different DMF content), applied voltage and tip–collector distance on fiber diameter and morphology were investigated. The diameter of fibers increased with the increase in the polymer concentration and decrease in the DMF content significantly. Applied voltage and tip–collector distance were found critical to control ‘bead’ formation. Elongation-at-break, ultimate strength and Young’s modulus were obtained from the mechanical tests, which were all increased by increasing fiber diameter. The fiber diameter significantly influenced both *in vitro* degradation (performed in Ringer solution) and *in vivo* biodegradation (conducted in rats) rates. *In vivo* degradation was found to be faster than *in vitro*. Electrospun membranes were more hydrophobic than PCL solvent-casted ones; therefore, their degradation was a much slower process.

Key words: Poly(ϵ -caprolactone); electrospinning; nanofibers; non-woven materials; degradation.

*To whom correspondence should be addressed. Tel.: (90-312) 440-6214. Fax: (90-312) 440-6214. E-mail: piskin@hacettepe.edu.tr

INTRODUCTION

During the last decade poly(α -hydroxy acids), mainly lactide and glycolide homo- and co-polymers, have received special and much interest among biodegradable polymers because of their proven and potential use in the medical and pharmaceutical field [1, 2]. Poly(ϵ -caprolactone) (PCL), a semi-crystalline biodegradable polyester, belongs to this family, and especially its co-polymers with lactides and glycolide are attracting increasing attention due to their controllable biodegradation rates in the desirable ranges (usually slower) and also more suitable and tailor-made mechanical properties (usually more flexible and softer) for some applications such as long-term drug delivery, and tissue repair and regeneration [3–20]. Several approaches have been investigated to produce biodegradable materials from PCL and its co-polymers, both porous and nonporous with different shapes in these studies.

One novel method of processing of biodegradable polymers including poly (α -hydroxy acids) is electrospinning, which is a unique method that produces polymer fibers with usually diameters in nanoscale and non-woven fibrous structures composed of these fibers [21–24]. The processing of biomaterials by conventional means (such as film casting and foaming) often imposes several limitations in the optimization of their final properties. The PCL cast films are not suitable for cell scaffolding because they are not porous and cannot facilitate the transport of nutrients and oxygen to the cells. In addition, the cast films can be too brittle to be handled. Electrospun non-woven materials have small pore size, high porosity and high surface area; therefore, they can be used in a wide variety of biomedical applications, such as for scaffolds in tissue engineering [25–27].

Yoshimoto *et al.* selected electrospinning to prepare PCL-based microporous, non-woven scaffolds and cultured mesenchymal stem cells derived from the bone marrow of neonatal rats on these electrospun scaffolds in the bioreactors, and suggested that these scaffolds are among the potential candidates for bone tissue engineering [28]. Lee *et al.* prepared nano-structured PCL non-woven mats by electrospinning for possible use as tissue-engineering scaffolds, and characterized their morphology, crystallinity and mechanical properties with different techniques [29]. Recently, novel, three-dimensional, nanofibrous PCL scaffolds composed of electrospun nanofibers have been evaluated as chondrocytes carrying scaffolds for possible cartilage repair by Li *et al.* [30]. These nanofibrous scaffold also supported cellular proliferation as evidenced by a 21-fold increase in cell growth over 21 days. They have concluded that the PCL nanofibrous structure may be a suitable candidate scaffold for cartilage tissue engineering.

Recently, we have also attempted to prepare non-woven fibrous biodegradable materials from poly(α -hydroxy acids), which were synthesized in our labs with different molecular weights and chain structures, using electrospinning [31]. In this study we report the synthesis of PCL and its processing into nanofibers and fibrous non-woven structures by electrospinning under different conditions, and *in vitro*

and *in vivo* degradation of these electrospun PCL materials. Another study related to application of these materials for prevention of post-surgery-induced abdominal adhesion in rats was reported elsewhere [32].

MATERIALS AND METHODS

Polymer synthesis and characterization

ϵ -Caprolactone (Aldrich, Germany) was dried on a molecular sieve for about 24 h. The catalyst, stannous octoate (Sigma, USA), and other agents were analytical grade and used as received. The polymerization system and procedure were described in detail elsewhere [33]. Briefly, polymerization was performed in the glass reactor under nitrogen atmosphere for 24 h at 120°C. The monomer/catalyst ratio was 1700 : 1 (mol/mol) in homo-polymerization of caprolactone. Low-molecular-weight residuals were removed by a dissolution–precipitation method in which chloroform and methanol were used as the solvent and precipitant, respectively.

The number and weight average molecular weights (M_n and M_w) and polydispersity index (PI) were determined by gel-permeation chromatography (GPC; Shimadzu, LC 10A, Japan) in chloroform at ambient temperature. Molecular weight of the polymer was determined relative to narrow molecular weight polystyrene standards.

FT-IR spectra was used for chemical characterization of polymer (and its purity), which were recorded by a FT-IR spectrophotometer (Shimadzu, DR8101, Japan). The polymer sample was dissolved in chloroform with a concentration of about 5% (w/v). Potassium bromide tablets were coated with this solution to form very thin films. The FT-IR spectra of the electrospun materials were recorded by using the ATR attachment of the equipment.

The $^1\text{H-NMR}$ spectra were recorded with a NMR spectrophotometer (Varian, Unity Inova, USA). The polymer was dissolved in CDCl_3 (5 mg polymer in 1 ml) and the spectra were recorded at 500 MHz and at a constant temperature of 18°C.

The thermal transitions of the polymer were obtained by a differential scanning calorimeter (DSC, Netzsch DSC 204, Germany) at a heating rate of 10°C/min from –100 to 100°C, under a nitrogen flow as a sweeping gas (100 ml/min).

The X-ray analyses were done using an X-ray diffractometer (Bruker AXS, D8 Advance, USA) in θ – 2θ -locked couple mode between 2θ angles of 10° and 90°, with a step size of 0.02 and step duration of 1 s. The X-ray generator was operated at 40 kV and 40 mA.

Electrospinning

The electrospinning system (see Fig. 1) that was used in this study was a home-made system consists of: (i) a high voltage (HV) power supply (CPS, 2594, USA) which can generate voltages of up to 50 kV with 500 μA direct current; (ii) a glass

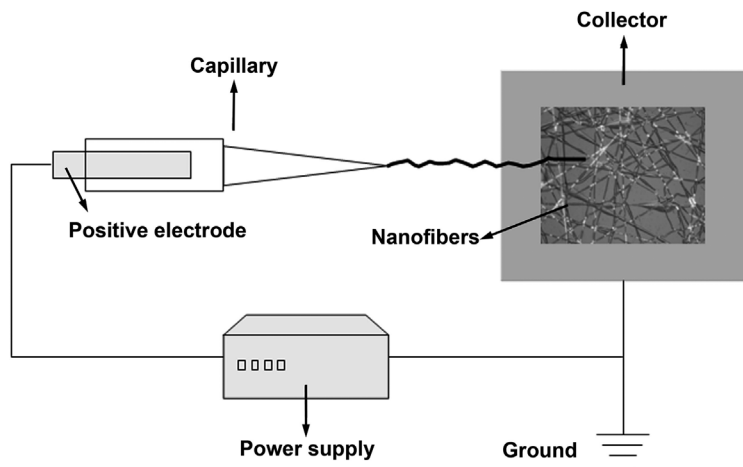


Figure 1. Schematic description of the electrospinning system used and a typical PCL nanofiber structure formed on the collector.

capillary in which a copper probe is inserted. The diameters of the capillary and its tip were 5 and 1 mm, respectively; and (iii) a collector which is a grounded aluminum sheet.

Non-woven PCL materials were electrospun from the solutions of PCL in mixtures of chloroform (C) and N,N-dimethyl formamide (DMF). In a typical experiment, the polymer solution was placed in the glass capillary. The copper probe of the HV generator was inserted into the capillary. The grounded aluminum sheet was positioned opposite to the tip of the capillary. The electrical field was applied and electricity was conducted through the solution. The output voltage and the current between the copper probe and the grounded aluminum sheet were measured. The fluid jet was ejected from the capillary. As the jet accelerated towards the grounded collector, the solvent evaporated and the polymer fibers were deposited on the collector in the form of a non-woven fabric.

In order to control the fiber dimensions, bead formation and final structure of the non-woven materials, we changed either the PCL concentration (4–15 g/100 ml), the DMF volume percentage in the solvent mixture (0–90%), the applied voltage (13–30 kV) or the capillary tip–collector distance (5–20 cm).

The fiber diameter and polymer morphology of the electrospun nanofibrous structures were investigated using an optical microscope (Eclipse ME600, Nikon, Japan) and a scanning-electron microscope (Supra 35VP, LEO, USA). The SEM images were taken after depositing the electrospun films with a conductive coating of gold with a sputter coater (K950X, Emitech, USA).

For the determination of wettability (or hydrophobicity), the contact angle of the electrospun non-woven materials and solvent casted PCL films were measured by a Digital Contact Angle Measurement system (CAM 100, KSV, Finland). The sample material was first attached to the glass slide with the aid of a double-sided tape and

then a small distilled water droplet (≈ 5 mg in weight) was carefully placed along the sample. Images of the droplet were automatically taken. From these images, the contact angle values were calculated.

For mechanical tests a Universal Test Machine (LR 5K, Lloyd Instruments, UK) was used. The specimens that were cut from the non-woven matrices (0.5×5 cm in size and approximately $15 \mu\text{m}$ in thickness) were utilized in the tests in which a cross-head speed of 5 mm/min at room temperature was applied.

In vitro degradation

The electrospun non-woven materials produced in the previous step were cut into specimens (0.5×5 cm in size and approximately $15 \mu\text{m}$ in thickness). For *in vitro* degradation tests, these specimens were placed into sterile (autoclaved) flasks (250 ml) containing 100 ml of pH 7.4 Ringer solution (Eczacıbaşı-Baxter, Turkey). The flasks were stirred gently at 37°C for 6 months. The samples were taken from the flasks at different time intervals (1st, 2nd, 3rd and 6th month). Before the characterization, the samples were first rinsed several times with distilled water and then dried in vacuum at room temperature.

The changes in average molecular weights (both M_n and M_w), molecular weight distributions (PI) and in mechanical properties (i.e., elongation-at-break, ultimate strength and Young's modulus) were determined as described above.

In vivo degradation

Thirty Wistar-Albino female rats weighing 250–300 g were used. All rats were fed with laboratory chow and water *ad libitum*. They were maintained in a temperature and humidity controlled environment at the Animal Research Department of Hacettepe University. The following biodegradation tests were applied after receiving permission/approval from the Animal Ethical Committee of the University.

Sterile surgical technique was applied throughout the study. The electrospun PCL materials were sterilized by γ -irradiation (2.5 Mrad). Animals were anesthetized by intraperitoneal injection with a mixture of ketamine HCl (50 mg/ml, Parke Davis, Taiwan) and Rompun (2%, Bayer, Germany). An area of about 3 cm^2 in the back of the test animal was shaved and disinfected with Baticon solution (10%, Drokstan, Turkey). A longitudinal incision (approximately 3 cm long) was made in this region using a blade (No. 11). Subcutaneous pockets were created by incision using blunt scissors. After implanting the non-woven PCL samples (2×1.5 cm) subdermally, the incision was closed with 5–0 silk sutures. PCL materials were withdrawn from the animals at selected time intervals (after 15, 30, 45 and 90 days post-implantation). They were rinsed with ethanol/water (70 : 30, v/v) and distilled water, and then vacuum dried at room temperature overnight. The degree of degradation was followed by measuring the average molecular weights and molecular weight distribution of the polymer using GPC as described before.

RESULTS AND DISCUSSION

Properties of PCL

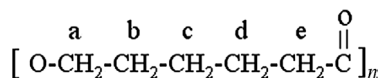
The homo-polymer of ϵ -caprolactone was synthesized by ring-opening polymerization in bulk with stannous octoate as the catalyst. The number (M_n) and weight (M_w) average molecular weights and the molecular weight distribution as polydispersity indices ($PI = M_w/M_n$) of the polymers before and after electrospinning obtained by GPC are 51 682 and 51 172; 85 741 and 84 387; and 1.65 and 1.64, respectively, showing that there is no significant degradation in polymer induced by the electrospinning process.

The characteristic peaks in FT-IR spectra of PCL before and after electrospinning were almost the same, which are as follows: 1733–1725 cm^{-1} for $-\text{C}=\text{O}$ stretching; 1295–1164 cm^{-1} for $-\text{C}-\text{O}$ stretching; 1419–1367 cm^{-1} for $\text{C}-\text{H}$ bending and 2865–2359 cm^{-1} for $\text{C}-\text{H}$ stretching, as also reported in the related literature [34, 35].

The following characteristic peaks corresponding to the H atoms at different positions on the caprolactone monomer (see Scheme 1) were observed in the $^1\text{H-NMR}$ spectra of both the virgin polymer (before electrospinning) and electrospun PCL: 4–4.2, 1.4–1.7, 1.2–1.4 and 2.2–2.4 ppm, for the protons a, b, c, d and e, respectively, which were similar to values reported in the literature [36–38]. There was no extra peak on the electrospun PCL spectrum; therefore, we assume that there is no degradation and product is quite pure.

The glass transition temperature (T_g) and melting temperature (T_m) of both the virgin polymer and its electrospun form were found from the DSC thermograms, and were -62°C and 69.5°C ; and -62°C and 61.9°C , respectively. The significant decrease in the melting temperature of PCL after electrospinning could be attributed to the decrease in the overall crystallinity of the electrospun PCL, which has been discussed in the related literature [39].

In order to further investigate the retardation of the crystallinity due to the electrospinning process as reported also by Lee *et al.* [29], Deitzel *et al.* [39] and Zong *et al.* [40] in their related publications, we performed X-ray analyses. Figure 2 shows the XRD patterns for both the virgin and electrospun PCL. As seen here, the peak positions in each diffraction pattern are essentially identical, showing that there is no change in crystal structure induced by the electrospinning of PCL as also reported by Lee *et al.* [29]. However, it is immediately evident that the diffraction peaks associated with the PCL synthesized are sharp while, the peaks in the pattern from the non-woven material are broader, indicating that the crystallinity of the electrospun PCL non-woven materials was lower than those for the virgin PCL



Scheme 1.

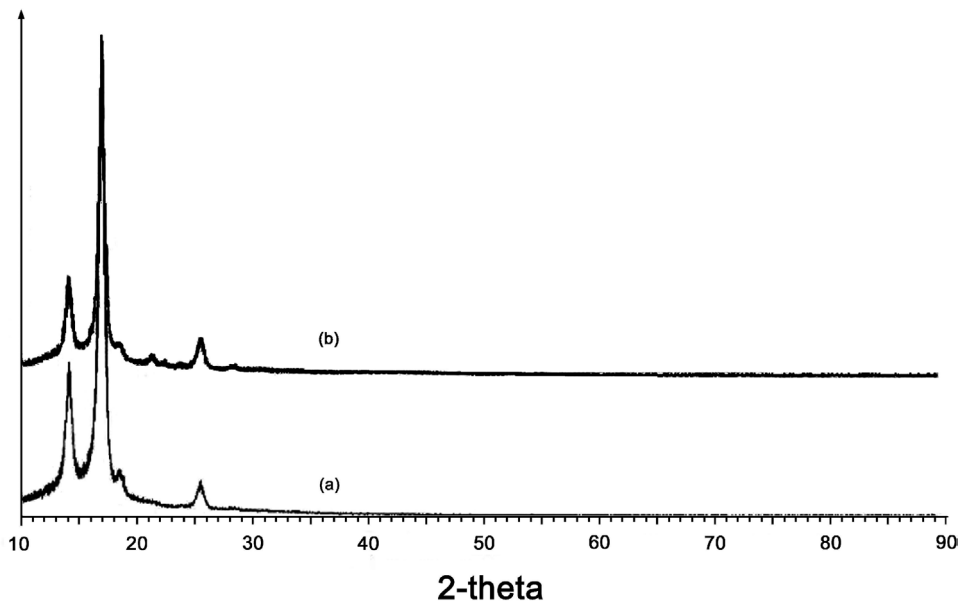


Figure 2. Representative XRD patterns: (a) the virgin PCL synthesized and (b) electrospun PCL.

synthesized in this study. These findings again confirmed that crystallization was retarded during electrospinning, which could be attributed to the retardation effect on crystallization due to rapid solidification of the stretched chains. According to Zong *et al.* [41], the stretched chains did not have enough time to organize into 3D-ordered crystal structures before they were solidified in electrospinning.

Structure and properties of electrospun PCL materials

In electrospinning several factors, including polymer type, molecular weight and its distribution, initial polymer concentration, polymer solution properties (viscosity, surface tension, compatibility with polymer, etc.), the applied voltage, capillary properties and its distance from the collector system, environmental condition that the fiber jet moves in and collector system, do affect the fiber diameter which, in turn, changes the bulk properties of the non-woven matrices formed from these fibers and also bead formation, which is not desirable in most cases [39, 42–45]. In order to produce fibers with different diameters with reduced bead formation, considering the results in the related literature, we changed the solution composition, applied voltage and tip–collector distance. Figure 3a and 3b gives representative SEM images of two electrospun materials, one almost without any bead formation and the other with a large number of beads, respectively.

In the first group, only PCL concentration in the feed was changed between 4 and 15 g/100 ml, while the other parameters, the DMF volume percentage, applied voltage and tip–collector distance were kept constant at 70%, 13 kV and 10 cm, respectively. The fiber diameter increased with increasing PCL concentration, from

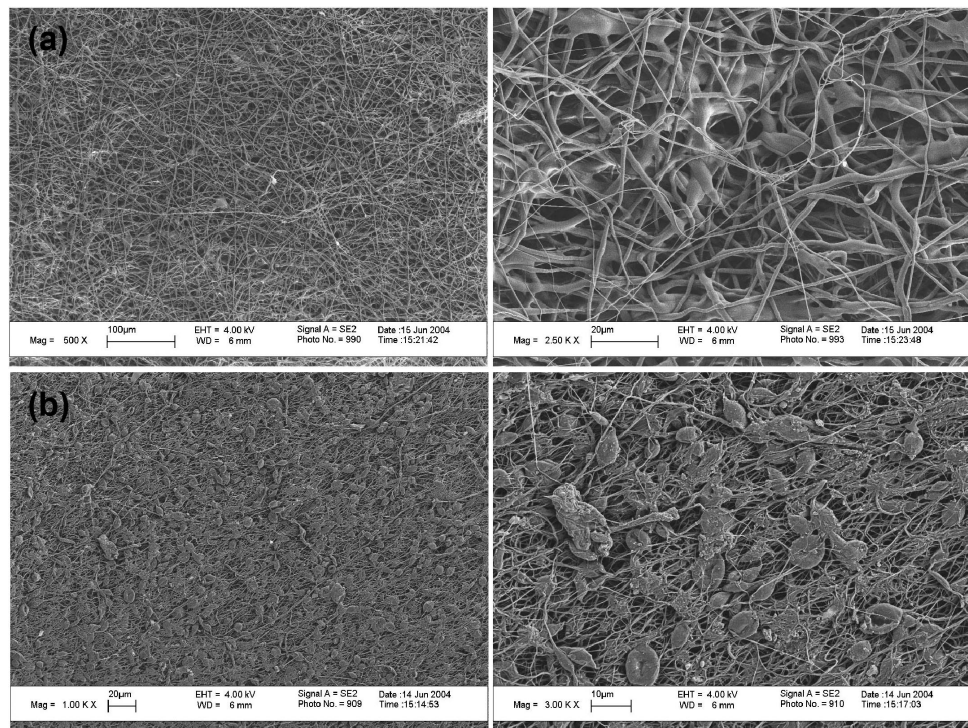


Figure 3. Representative SEM micrographs of two samples: (a) almost without any bead and (b) with many beads. Both at two different magnifications.

Table 1.

Effects of polymer concentration on fiber diameter and bead formation

Polymer (g/100 ml)	Average fiber diameter* (nm)	Bead formation
4	52 ± 10	Many beads
6	59 ± 10	Many beads
8	66 ± 10	Many beads
10	80 ± 10	Many beads
13	93 ± 10	Few beads
15	250 ± 10	Almost no beads

*The average diameter of a minimum of 10 fibers at different points ± SD.
DMF content: 70%; applied voltage: 13 kV; tip-collector distance: 10 cm.

50 nm to around 100 nm until a PCL concentration of 13 g/100 ml, thereafter there was a very significant increase from 100 nm to 250 nm by increasing the PCL concentration only from 13 to 15 g/100 ml (Table 1). Similar results were reported by others. Deitzel *et al.* pointed out that the fiber diameter increased with increasing polymer concentration [39]. Demir *et al.* reported that fiber diameter was proportional to the cube of polymer concentration [44]. Note that there was a large amount of beads in the structure when reduced PCL concentration lower than

Table 2.

Effects of DMF content on fiber diameter and bead formation

DMF (vol%)	Average fiber diameter* (nm)	Bead formation
90	196 ± 15	Almost no beads
70	250 ± 15	Almost no beads
40	300 ± 20	Almost no beads
30	689 ± 30	Almost no beads
0	1297 ± 35	No beads

*The average diameter of a minimum of 10 fibers at different points ± SD.

Polymer concentration: 13 g/100 ml; applied voltage: 13 kV; tip–collector distance: 10 cm.

10 g/100 ml. Fong *et al.* reported also that higher polymer concentrations result in fewer beads in the electrospun matrices [45].

Solvent type has also been found to be one of the important parameters, influencing not only the fiber diameter but also bead formation [29, 46]. In the initial studies we used pure chloroform, which is a good solvent for PCL; however, the fibers that we produced exhibited diameters in micron size level. Note that our aim was to produce fibers with a diameter in the nanometer range. Therefore, in order to reduce the diameter we included DMF in the solvent mixture and increased its volume percentage up to 90%. The effect of DMF content (as DMF volume percentage) on the fiber diameter is given in Table 2. Note that in this group of experiments the PCL concentration in the feed, applied voltage and tip–collector distance were kept constant at 13 g/100 ml, 13 kV and 10 cm, respectively. As seen here there was a very steep decrease in diameter from about 1300 nm to 300 nm, when we included DMF in the solvent mixture up to 40%, thereafter the decrease was not significant. We were able to eliminate bead formation especially using solvent mixtures with DMF content more than 40%. Note that addition of DMF not only changes the compatibility of the solvent system with PCL, but also affects solvent properties; therefore, both fiber dimensions and bead formation. Lee *et al.* investigated the effects of solution properties (i.e., surface tension, viscosity, dielectric constant and conductivity) using solvent mixtures including methylene chloride, DMF and toluene with different ratios on both fiber diameter of PCL electrospun fibers and also bead formation [29]. Doshi *et al.* pointed out that by reducing surface tension of a polymer solution, fibers could be obtained without beads [42].

In this group of studies we also changed the applied electrospinning voltage in the range 13–30 kV, while the PCL concentration, DMF volume percentage and tip–collector distance were kept constant at 13 g/100 ml, 70% and 10 cm, respectively. As seen in Table 3 the average fiber diameter increased with increasing applied voltage, although the influence was not as great as those observed in the previous group of studies discussed above. Note that significant bead formation was observed with increasing applied voltage. There are some reports about the effects of voltage in the literature stating the opposite, i.e., that the fiber diameter decreases with the applied voltage [47, 48].

Table 3.

Effects of applied voltage on fiber diameter and bead formation

Applied voltage (kV)	Average fiber diameter* (nm)	Bead formation
13	93 ± 10	Few beads
20	99 ± 5	More than a few beads
25	105 ± 5	More than a few beads
30	115 ± 5	Many beads

*The average diameter of a minimum of 10 fibers at different points ± SD. Polymer concentration: 13 g/100 ml; DMF content: 70%; tip–collector distance: 10 cm.

We also changed the capillary tip–collector distance between 5–20 cm by keeping the PCL concentration, DMF volume percentage and applied voltage constant at 13 g/100 ml, 70% and 13 kV, respectively. It was found that, although the fiber size did not change significantly, homogeneously distributed beads started to form along PCL fibers when reducing the distance, as also stated by Megelski *et al.* [48].

Mechanical properties of electrospun materials

The electrospun PCL non-woven materials exhibit quite different appearance and physical properties, very different than a PCL cast film. They are opaque, light, soft and flexible, like a butterfly wing or a very soft human skin, but quite strong materials that may have great potential to be used as a wound dressing, because they very tightly take the shape of the part of the body that they are placed on. These properties are already under investigation in our group [32].

In this section, we report the mechanical properties of some selected PCL materials prepared under different conditions, discussed in the previous section, by using a universal test machine. A typical stress–strain curve obtained is given in Fig. 4, which is used to determine the mechanical properties, i.e., elongation at break, ultimate strength and Young's modulus. Tables 4 and 5 give the data obtained. Note that these values are the average of minimum 3 measurements carried out on the same specimens prepared using PCL solutions either with different concentrations (with a DMF volume percentage of 70%) or with different DMF contents (with a PCL concentration of 15 g/100 ml), were evaluated. In these experiments, the applied voltage and tip–collector distance were 13 kV and 10 cm in all cases and the thickness of the non-woven materials was about 15 μm.

As discussed in the previous sections, and as also seen in Tables 4 and 5, fiber diameter forming during electrospinning changes quite significantly with both an increase in the PCL concentration and with a decrease of the DMF content. Note also that the fiber microstructure forming the material (especially bead formation, fiber orientation, etc.) and also polymer morphology (crystallinity, molecular orientation, etc.) within the fibers would also be different in the materials produced at different conditions. The important point observed Tables 4 and 5 is that, interestingly, elongation-at-break, ultimate strength as well as Young's modulus increase with the increase in the fiber diameter. Note also that the matrices formed

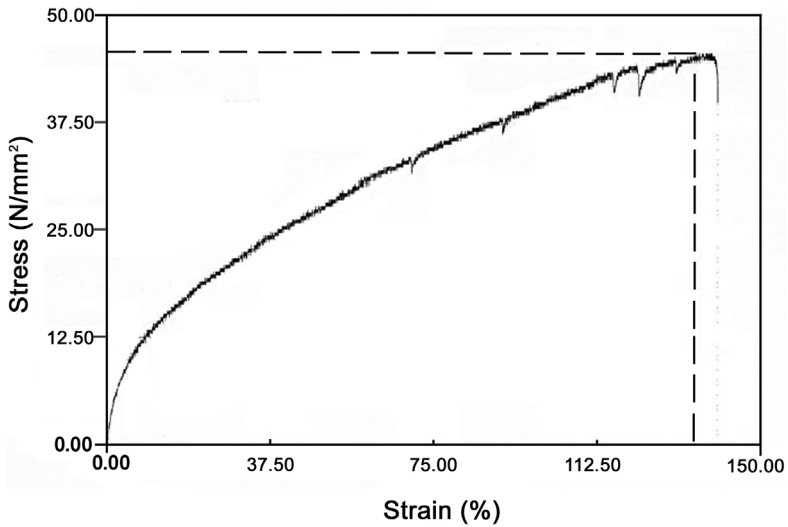


Figure 4. A representative stress–strain curve of electrospun PCL material.

Table 4.

Mechanical properties of some selected PCL non-woven materials prepared using polymer solutions with different polymer concentrations

Polymer (g/100 ml)	Average fiber diameter (nm)	Elongation-at-break (%)	Ultimate strength (MPa)	Young's modulus (MPa)
4	52 ± 10	9.7	4.6	0.6
6	59 ± 10	16.7	5.3	0.7
8	66 ± 10	18.4	5.6	0.8
10	80 ± 10	22.2	7.8	4.1
13	93 ± 10	69.0	16.6	3.7
15	250 ± 10	110.0	16.6	4.4

The values are the average of 3 tests performed on each specimen. Standard deviations for elongation-at-break, ultimate strength and Young's modulus were less than ±7.8, ±4.3 and ±1.2, respectively.

Table 5.

Mechanical properties of some selected PCL non-woven materials prepared using solvent mixtures with different DMF contents

DMF (vol%)	Average fiber diameter (nm)	Elongation-at-break (%)	Ultimate strength (MPa)	Young's modulus (MPa)
90	196 ± 15	82.0	17.4	3.5
70	250 ± 15	110.0	16.6	4.4
40	300 ± 20	139.0	45.8	3.5
30	689 ± 30	150.1	48.9	4.2

The values are the average of 3 tests performed on each specimen. Standard deviations for elongation-at-break, ultimate strength and Young's modulus were less than ±7.8, ±4.3 and ±1.2, respectively.

from thicker fibers contain fewer beads. The matrices with finer fibers are much weaker than those observed for mats with thicker fibers, which is most probably due to many beads in the case of finer fibers. Interestingly, materials become more flexible, but at the same time stronger and harder when the fiber diameter is increased and less beads are formed. This is a unique mechanical property that can be reached with electrospinning, as also discussed by Zong *et al.* [41]. Huang *et al.* reported also that the beads on fiber surface might have considerably reduced the cohesive force between the fibers of the non-woven fiber mat and, hence, a poorer mechanical performance of the nanofiber mat was obtained [49].

In vitro degradation behavior

In vitro degradation of electrospun PCL non-woven materials was investigated in Ringer solution at 37°C for a period of 6 months. Degradation was followed by measuring the changes in mechanical properties and molecular weights and distribution. Tables 6–11 give the changes in elongation-at-break, ultimate strength and Young's modulus, respectively. These tests were performed only on some selected materials prepared using PCL solutions either with different concentrations

Table 6.

Changes in elongation-at-break (in %) of some selected PCL non-woven materials prepared using polymer solutions with different PCL concentrations due to *in vitro* degradation

Polymer (g/100 ml)	Average fiber diameter (nm)	Degradation time (months)				
		0	1	2	3	6
4	52 ± 10	9.7	10.6	3.5	3.5	N/A
6	59 ± 10	16.7	15.2	6.3	N/A	N/A
13	93 ± 10	69.0	62.6	47.0	36.7	22.8
15	250 ± 10	110.0	88.0	47.0	34.8	19.4

Values are the average of 3 tests performed on each specimen and standard deviations were less than ±7.8. N/A, these materials were very weak and brittle; therefore, the mechanical test was not applied.

Table 7.

Changes in elongation-at-break (in %) of some selected PCL non-woven materials prepared using solvent mixtures with different DMF contents

DMF (vol%)	Average fiber diameter (nm)	Degradation time (months)				
		0	1	2	3	6
90	196 ± 15	82.0	38.0	32.0	42.3	5.7
70	250 ± 15	110.0	88.0	47.0	34.8	19.4
40	300 ± 20	139.0	130.1	125.8	87.4	50.1
30	689 ± 30	150.0	130.0	128.2	125.0	122.2

Values are the average of 3 tests performed on each specimen and standard deviations were less than ±7.8. N/A, these materials were very weak and brittle; therefore, the mechanical test was not applied.

(with a DMF volume percentage of 70%) or with different DMF content (with a PCL concentration of 15 g/100 ml), were evaluated. The applied voltage and tip–collector distance were 13 kV and 10 cm, respectively, in all cases and the thicknesses of the non-woven materials were about 15 μm.

As seen in Tables 6–11, there is a clear tendency, which is the decrease in the elongation-at-break, ultimate strength and Young’s modulus values for all of the materials tested in this section. The materials become less flexible (even very brittle in some cases) and mechanically weak, as expected due to degradation. During the degradation period, samples with different diameters showed decrease in mechanical properties with different rates, depending on the fiber diameter. The thinner fibers had a greater degradation rate in comparison to the thicker one. A possible explanation of the different degradation behavior of the PCL samples having different fiber diameters is related to their surface to volume ratio. Note that, most probably, geometrical (e.g., size, shape and surface to volume ratio) and morphological (e.g., existence of beads) factors also influenced the degradation. A high surface to volume ratio means high water penetration, which leads to high degradation rates.

Table 8.

Changes in ultimate strength (in MPa) of some selected PCL non-woven materials prepared using polymer solutions with different polymer concentrations due to *in vitro* degradation

Polymer (g/100 ml)	Average fiber diameter (nm)	Degradation time (months)				
		0	1	2	3	6
4	52 ± 10	4.55	43.05	35.35	19.53	N/A
6	59 ± 10	5.22	48.54	48.27	N/A	N/A
13	93 ± 10	16.58	24.16	13.38	17.42	16.53
15	250 ± 10	17.38	24.16	17.42	13.38	10.54

Values are the average of 3 tests performed on each specimen and standard deviations were less than ±4.3. N/A, these materials were very weak and brittle; therefore, the mechanical test was not applied.

Table 9.

Changes in ultimate strength (in MPa) of some selected PCL non-woven materials prepared using solvent solutions with different DMF content due to *in vitro* degradation

DMF (vol%)	Average fiber diameter (nm)	Degradation time (months)				
		0	1	2	3	6
90	196 ± 15	17.40	17.67	18.84	16.29	5.02
70	250 ± 15	17.38	24.16	17.42	13.38	10.54
40	300 ± 20	45.75	50.10	38.97	25.39	22.11
30	689 ± 30	48.94	38.22	18.25	27.03	31.90

Values are the average of 3 tests applied on each specimen and standard deviations were less than ±4.3.

Table 10.

Changes in Young's modulus (in MPa) of some selected PCL non-woven materials prepared using polymer solutions with different polymer concentrations due to *in vitro* degradation

Polymer (g/100 ml)	Average fiber diameter (nm)	Degradation time (months)				
		0	1	2	3	6
4	52 ± 10	0.6	4.4	3.3	0.6	N/A
6	59 ± 10	0.7	9.0	44.4	N/A	N/A
13	93 ± 10	3.7	3.3	3.3	3.2	1.1
15	250 ± 10	4.4	3.4	3.2	2.8	1.3

Values are the average of 3 tests applied on each specimen and standard deviations were less than ±1.2. N/A, these materials were very weak and brittle; therefore, the mechanical test was not applied.

Table 11.

Changes in Young's modulus (in MPa) of some selected PCL non-woven materials prepared using solvent mixtures with different DMF content due to *in vitro* degradation

DMF (vol%)	Average fiber diameter (nm)	Degradation time (months)				
		0	1	2	3	6
90	196 ± 15	3.5	2.9	2.6	1.9	1.0
70	250 ± 15	4.4	3.4	3.2	2.8	1.3
40	300 ± 20	3.5	2.0	1.8	1.8	2.5
30	689 ± 30	4.2	3.3	3.2	2.7	2.7

Values are the average of 3 tests applied on each specimen and standard deviations were less than ±1.2.

Figure 5 gives the changes in the weight-average molecular weight (M_w) of some selected electrospun PCL materials that were prepared by changing the DMF content. Here, PCL initial concentration, applied voltage and tip-collector distance were 15 g/100 ml, 13 kV and 10 cm, respectively, and the thickness of the non-woven materials was about 15 μ m. As seen in Fig. 5, the thinner fibers had a higher degradation rate in comparison to thicker one which is parallel to the results of degradation behavior observed in the mechanical tests. Most probably not only fiber dimensions but also existence of beads affected degradation behavior. The PI values did not change significantly with degradation; therefore, the decreases in the number-average molecular weights (M_n) were in parallel to the data presented in Fig. 5 for M_w .

In our previous studies, we have produced PCL films by solvent casting and investigated their *in vitro* degradation in the same medium and under the same conditions. The results have been reported elsewhere [50]. For instance, the decrease in M_w of solvent-cast PCL film was about 29% in two months, while the decrease was only 5% in the case of electrospun PCL non-woven material. The degradation process of aliphatic polyesters is based on a hydrolytic reaction [51, 52]. They have ester bonds on their backbone (main) chains which are cleaved by the reaction

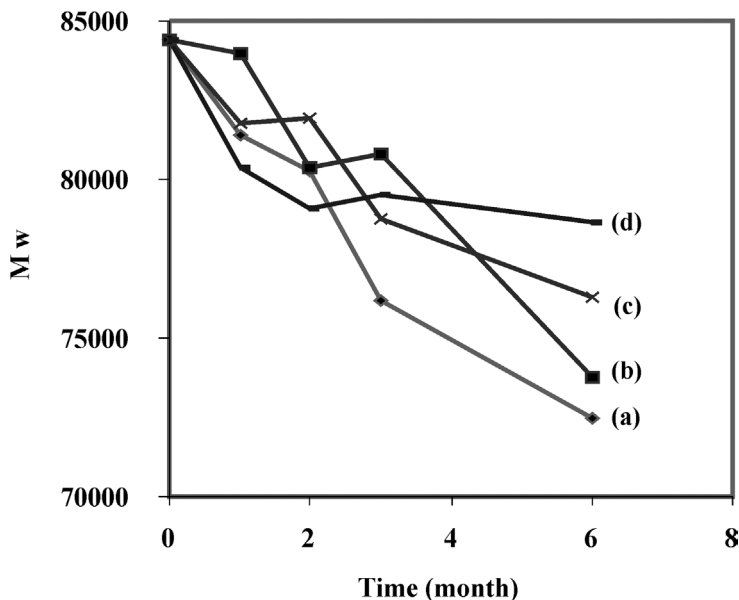


Figure 5. Changes in M_w with time due to degradation for PCL materials prepared with different DMF contents: (a) 90% (fiber diameter 196 nm); (b) 70% (fiber diameter 250 nm); (c) 40% (fiber diameter 300 nm); (d) 30% (fiber diameter 689 nm).

with water. When the water molecules attack the ester bonds in the polymer chains, the average length of degraded chains becomes shorter. Eventually, the process results in short fragments of chains having carboxyl end-groups that become soluble in water. As a result the degradation products will lower the local pH value and catalyze the degradation rate. The degradation products (both oligomers and monomers) carrying carboxylic acid end-groups in the case of degradation of ϵ -caprolactone homo-polymer are responsible for the autocatalytic bulk degradation of the material made of this polymer, in which degradation rate is even much faster than ordinary hydrolysis [52–54]. Kim *et al.* suggested that electrospun materials are fibrous structures, where the dimension of the nanofiber is small and the diffusion length for the degraded by-products is short, the hydrophilic oligomers can quickly escape from the surface and, therefore, the possibility of autocatalysis in electrospun membranes is very limited [55]. This conclusion may also be an explanation in our case, in which degradation of electrospun PCL was much slower than those observed with solvent cast.

However, in addition we have measured the contact angles of both electrospun non-woven materials and solvent casted nonporous films prepared from the same PCL that we have produced in this study. The contact angles of the electrospun and solvent-cast PCL material were 98° and 71° , respectively. It means that electrospun PCL materials were more hydrophobic; this may be a result of fiber (and, therefore, non-woven matrix) formation during electrospinning, which resulted in different surface morphology and, thus, different degree of wettability. It is expected that

more hydrophobic polymer matrices are degraded at slower rates and from the surface, mainly because of low water penetration rates, as also observed in our case, which is another explanation for the slower degradation rates in the case of electrospun PCL materials.

In vivo degradation behavior

After concluding the results of the studies discussed above we selected one of the non-woven PCL materials to carry on further investigation considering potential medical use as, e.g., wound dressing and guided tissue-regeneration materials. The M_w , M_n and PI ($= M_w/M_n$) of the polymer used to prepare this material were obtained by GPC and were 84 387, 51 172 and 1.64, respectively. This material was prepared by using a PCL solution in a mixture of chloroform and DMF with a PCL concentration of 13 g/100 ml and a DMF content of 70%. The applied voltage and tip–collector distance were 13 kV and 10 cm, respectively. The elongation-at-break, ultimate strength and Young’s modulus of this fibrous material (with a thickness of 15 μm) were 69.0%, 16.6 MPa and 3.7 MPa, respectively.

Several specimens (2×1.5 cm) were cut from this non-woven PCL material and implanted in rats as described in the previous sections. They were withdrawn from the animals at selected time intervals (15, 30, 45 and 90 days post-implantation), cleaned and then vacuum-dried at room temperature overnight. Note that, since it was not possible to remove the biological residues that had penetrated in the matrix, we decided not to apply mechanical tests in these degradation tests. We only dissolved the polymer phase and then followed the changes in M_w , M_n and PI of the polymer by GPC (see Table 12).

At the end of the implantation period of 90 days, the M_w of the material had decreased by 27%. At the same time, the PI increased, indicating an active chain scission of the polymer. After *in vitro* degradation, the electrospun PCL materials showed 4% M_w loss at the end of 90 days. The M_w loss profiles indicated faster degradation *in vivo* as compared with *in vitro*. Faster degradation rate *in vivo* may be due to several factors, including foreign body response. As a result of the *in vivo* implantation, the typical response results in the accumulation of cells, such as macrophages, around the foreign body leading to a walling of the region. Free radicals, acidic products, or enzymes produced by these cells during the foreign body response may accelerate degradation [56].

Table 12.

Changes of M_w , M_n and PI with time due to *in vitro* degradation

	<i>In vivo</i> degradation period (days)				
	0	15	30	45	90
M_w	84 387	73 381	70 993	74 294	61 200
M_n	51 172	44 589	43 189	45 961	35 956
PI	1.64	1.64	1.64	1.64	1.70

Note that, as reported in the related literature, aliphatic polyesters, including lactide and glycolide homo- and co-polymers, are mainly degraded by non-enzymatic random hydrolytic scission of esters linkage both *in vitro* and *in vivo* [38, 57, 58]. However, in the case of PCL enzymes might play a role to some extent [59]. Pitt *et al.* showed that PCL is degraded both *in vitro* and *in vivo* by simple hydrolysis, while enzymes also play a role in the degradation of the elastomeric co-polymers of ϵ -caprolactone with δ -valerolactone [53, 60]. Enzymatic degradation of PCL by various lipases was documented by Li *et al.* [61]. It was generally agreed that enzymes may play a role at the later stages of degradation when chains are fragmented; then the smaller fragments can be phagocytosed and degraded intracellularly [62, 63].

CONCLUSIONS

In this study non-woven PCL materials were prepared by electrospinning. The effects of four parameters, i.e., the initial PCL concentration, composition of the solvent mixture (or DMF content), tip-collector distance and applied voltage, on the nanofiber diameter and the fibrous material morphology were investigated. The first two parameters were found to be very effective on the fiber diameter which increased by increasing the PCL concentration and decreasing DMF content. The latter two parameters did not change the diameter very significantly, but were found to be critical on undesirable bead formation. Interestingly, materials become more flexible but stronger when the nanofiber diameter is increased. *In vitro* degradation studies performed in Ringer solution showed that PCL materials formed from thinner fibers degraded faster than those composed of thicker fibers. The main reason for the different degradation behavior was attributed to the different surface/volume ratio of the fibers. The molecular weight decrease during *in vitro* degradation of electrospun PCL materials were much lower than those previously reported for solvent casted PCL films, which may be due to diffusion of oligomers out of the fibers much easily (as a result of high surface/volume ratio) which reduced the effects of autocatalytic degradation. Results demonstrated that the electrospinning process decreased the surface hydrophilicity which reduces the water uptake and therefore hydrolytic degradation rate. Electrospun PCL materials were degraded much faster *in vivo* as compared with *in vitro*. The faster degradation rate *in vivo* may be due to the enzymatic degradation of PCL in addition to the hydrolytic degradation.

Acknowledgements

E. P. is supported by the Turkish Academy of Sciences as a full member.

REFERENCES

1. E. Pişkin, in: *Degradable Polymers: Principles and Applications*, G. Scott (Ed.), p. 321. Kluwer, Dordrecht (2002).
2. L. Fambri, C. Migliaresi, K. Kesenci and E. Pişkin, in: *Integrated Biomaterials Science*, R. Barbucci (Ed.), p. 119. Kluwer/Plenum, New York, NY (2002).
3. C. G. Pitt, in: *Biodegradable Polymers as Drug Delivery Systems*, M. Chasin and R. Langer (Eds), p. 71. Marcel Dekker, New York, NY (1990).
4. S. L. Ishaug-Riley, L. E. Okun, G. Prado, M. A. Applegate and A. Ratcliffe, *Biomaterials* **20**, 2245 (1999).
5. M. Ekholm, J. Hietanen, C. Lindqvist, J. Rautavuori, S. Santavirta and R. Suuronen, *Biomaterials* **20**, 1257 (1999).
6. K. G. Marra, J. W. Szem, P. N. Kumta, P. A. DiMilla and L. E. Weiss, *J. Biomed. Mater. Res.* **47**, 324 (1999).
7. M. F. Meek, W. F. A. Den Dunnen, J. M. Schakenraad and P. H. Robinson, *Microsurgery* **19**, 247 (1999).
8. E. S. Carlisle, M. R. Mariappan, K. D. Nelson, B. E. Thomes, R. B. Timmons, A. Constantinescu, R. C. Eberhart and P. E. Bankey, *Tissue Eng.* **6**, 45 (2000).
9. K. W. Ng, D. W. Hutmacher, J. T. Schantz, C. S. Ng, H. P. Too, T. C. Lim, T. T. Phan and S. H. Teoh, *Tissue Eng.* **7**, 441 (2001).
10. D. W. Hutmacher, J. T. Schantz, I. Zein, K. W. Ng, S. H. Teoh and K. C. Tan, *J. Biomed. Mater. Res.* **55**, 203 (2001).
11. A. Valero-Cabré, K. Tsironis, E. Skouras, G. Perego, X. Navarro and W. F. Neiss, *J. Neurosci. Res.* **63**, 214 (2001).
12. A. Şenköylü, E. Ural, K. Kesenci, A. Şimşek, Ş. Ruacan and E. Pişkin, *Int. J. Artif. Organs* **25**, 1174 (2002).
13. W. J. Lin and C. H. Lu, *J. Membr. Sci.* **198**, 109 (2002).
14. A. G. A. Coombes, E. Verderio, B. Shaw, X. Li, M. Griffin and S. Downes, *Biomaterials* **23**, 2113 (2002).
15. Q. P. Hou, D. W. Grijpma and J. Feijen, *Macromol. Rapid. Commun.* **23**, 247 (2002).
16. Q. P. Hou, D. W. Grijpma and J. Feijen, *Biomaterials* **24**, 1937 (2003).
17. Ö. A. Gürpınar, K. Tuzlakoğlu, M. A. Onur, A. Tümer, M. A. Serdar, N. Ünal and E. Pişkin, *J. Biomater. Sci. Polymer Edn* **14**, 589 (2003).
18. C. Kazımoglu, S. Bölükbaşı, U. Kanatlı, A. Şenköylü, C. Babaç, H. Yavuz and E. Pişkin, *Int. J. Artif. Organs* **26**, 804 (2003).
19. G. Ciapetti, L. Ambrosi, L. Savarino, D. Granchi, D. Cenni, N. Baldini, S. Pagani, S. Guizzardi, F. Causa and A. Giunti, *Biomaterials* **24**, 3815 (2003).
20. H. Aydın, A. Çalıklı and E. Pişkin, *J. Biocomp. Bioact. Polym.* **19**, 383 (2004).
21. Z. M. Huang, Y. Z. Zhang, M. Kotaki and S. Ramakrishna, *Composit. Sci. Technol.* **63**, 2223 (2003).
22. A. Frenot and I. S. Chronakis, *Curr. Opin. Colloid Interf. Sci.* **8**, 64 (2003).
23. L. Larrondo and R. S. J. Manley, *J. Polym. Sci. Polym. Phys. Edn* **19**, 909 (1981).
24. L. A. Smith and P. X. Ma, *Coll. Surf. B: Biointerfaces* **39**, 125 (2004).
25. W. Li, C. Laurencin, E. Caterson, R. Tuan and F. Ko, *J. Biomed. Mater. Res.* **60**, 613 (2002).
26. C. Y. Xu, R. Inai, M. Kotaki and S. Ramakrishna, *Biomaterials* **25**, 877 (2004).
27. X. M. Mo, C. Y. Xu, M. Kotaki and S. Ramakrishna, *Biomaterials* **25**, 1883 (2004).
28. H. Yoshimoto, Y. M. Shin, H. Terai and J. P. Vacanti, *Biomaterials* **24**, 2077 (2003).
29. K. H. Lee, H. Y. Kim, M. S. Khil, Y. M. Ra and D. R. Lee, *Polymer* **44**, 1287 (2003).
30. W. J. Li, K. G. Danielson, P. G. Alexander and R. S. Tuan, *J. Biomed. Mater. Res.* **67**, 1105 (2003).
31. N. Bölgen, MSc Thesis, Hacettepe University, Ankara (2003).

32. N. Bölgen, İ. Vargel, P. Korkusuz, Y. Menceloğlu and E. Pişkin, *J. Biomed. Mater. Res.* (2005) (submitted).
33. E. Ural, K. Kesenci, L. Fambri, C. Migliaresi and E. Pişkin, *Biomaterials* **21**, 2147 (2000).
34. P. Dubois, R. Jacobs, R. Jerome and P. Teyssie, *Macromolecules* **24**, 2266 (1991).
35. S. Jacobsen, H. G. Fritz, P. Degee, P. Dubois and R. Jerome, *Ind. Crops Prod.* **11**, 265 (2000).
36. M. Malin, M. Hiljanen-Vainio, T. Karjalainen and J. Seppala, *J. Appl. Polym. Sci.* **59**, 1289 (1996).
37. M. Hiljanen-Vainio, T. Karjalainen and J. Seppala, *J. Appl. Polym. Sci.* **59**, 1281 (1996).
38. H. Quian, J. Bei and S. Wang, *Polym. Degrad. Stabil.* **68**, 423 (2000).
39. J. M. Deitzel, J. Kleinmeyer, D. Harris and N. C. B. Tan, *Polymer* **42**, 261 (2001).
40. X. H. Zong, X. S. Kim, D. F. Fang, S. F. Ran, B. S. Hsiao and B. Chu, *Polymer* **43**, 4403 (2002).
41. X. H. Zong, S. Ran, D. Fang, B. Hsiao and B. S. Chu, *Polymer* **44**, 4959 (2003).
42. J. Doshi and D. H. Reneker, *J. Electrostat.* **35**, 151 (1995).
43. H. Fong, I. Chun and D. H. Reneker, *Polymer* **40**, 4585 (1999).
44. M. M. Demir, I. Yilgor, E. Yilgor and B. Erman, *Polymer* **43**, 3303 (2002).
45. H. Fong and D. H. Reneker, *J. Polym. Sci. B: Polym. Phys.* **37**, 3488 (1999).
46. H. Q. Liu and Y. L. Hsieh, *J. Polym. Sci. B: Polym. Phys.* **40**, 2119 (2002).
47. M. S. Khil, D. I. Cha, H. Y. Kim, I. S. Kim and N. Bahattarai, *J. Biomed. Mater. Res. B: Appl. Biomater.* **67**, 675 (2003).
48. S. Megelski, J. Stephens, B. D. Chase and J. Rabolt, *Macromolecules* **35**, 8456 (2002).
49. Z. M. Huang, Y. Z. Zhang, S. Ramakrishna and C. T. Lim, *Polymer* **45**, 5361 (2004).
50. H. Yavuz, C. Babaç, K. Tuzlakoglu and E. Pişkin, *Polym. Degrad. Stabil.* **75**, 431 (2002).
51. E. A. Schmidt, D. R. Flanagan and R. Linhardt, *Macromolecules* **27**, 743 (1994).
52. S. Li and S. McCarthy, *Biomaterials* **20**, 35 (1999).
53. L. Lu, C. A. Garcia and A. G. Mikos, *J. Biomed. Mater. Res.* **46**, 236 (1999).
54. I. Grizzi, H. Garreau, S. Li and M. Vert, *Biomaterials* **16**, 305 (1995).
55. K. Kim, M. Yu, X. Zong, J. Chiu, D. Fang, Y. S. Seo, B. S. Hsiao and M. Hadjiargyrou, *Biomaterials* **24**, 4977 (2003).
56. M. A. Tracy, K. L. Ward, L. Firouzabadian, Y. Wang, N. Dong, R. Quian and Y. Zhang, *Biomaterials* **20**, 1057 (1999).
57. A. Duda, T. Biela, J. Libiszowski, S. Penczek, P. Dubois, D. Mecerreyes and R. Jerome, *Polym. Degrad. Stabil.* **59**, 215 (1998).
58. T. Matsui, T. Nakamura and T. Tsuda, *J. Jpn. Soc. Biomater.* **11**, 330 (1993).
59. Z. Gan, D. Yu, Z. Zhong, Q. Liang and X. Jing, *Polymer* **40**, 2859 (1999).
60. C. G. Pitt, T. A. Marks and A. Schindler, *NIDA Res. Monogr.* **28**, 232 (1981).
61. S. M. Li, L. J. Liu, H. Garreau and M. Vert, *Biomacromolecules* **4**, 373 (2003).
62. S. C. Woodward, P. S. Brewer, F. Moatamed, A. Schindler and C. G. Pitt, *J. Biomed. Mater. Res.* **19**, 437 (1985).
63. B. F. Matlaga and T. N. Salthouse, *J. Biomed. Mater. Res.* **17**, 185 (1983).

Copyright of Journal of Biomaterials Science -- Polymer Edition is the property of VSP International Science Publishers. The copyright in an individual article may be maintained by the author in certain cases. Content may not be copied or emailed to multiple sites or posted to a listserv without the copyright holder's express written permission. However, users may print, download, or email articles for individual use.